Talanta 299 (2026) 129147

Contents lists available at ScienceDirect

Talanta

journal homepage: www.elsevier.com/locate/talanta

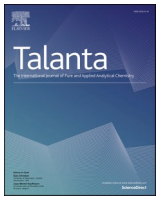

Improving electrochemical aptasensor sensitivity for *Bacillus cereus* spore detection in food safety applications

Milica Sentic [a,b], Francesco Rizzotto [a], Zorica Novakovic [c], Aleksandar Karajic [d], Brahim Heddi [e], Jasmina Vidic [a,*]

[a] Université Paris-Saclay, INRAE, AgroParisTech, Micalis Institute, Jouy en Josas, France
[b] University of Belgrade, Institute of Chemistry, Technology and Metallurgy, National Institute of the Republic of Serbia, Belgrade, Serbia
[c] University of Novi Sad, BioSense Institute, Novi Sad, 21000, Serbia
[d] Department of Electrical and Computer Engineering, Tufts University, Medford, 02155, MA, USA
[e] Laboratoire de Biologie et de Pharmacologie Appliquée, CNRS UMR8113, École Normale Supérieure Paris-Saclay, Gif sur Yvette, France

A B S T R A C T

Rapid detection of *Bacillus cereus* spores is essential for preventing food contamination and spoilage. Many existing methods detect *B. cereus* vegetative cells rather than spores and cannot be applied directly to foods. Here, we present a combination of aptamers targeting different moieties on the surface of *B. cereus* spores with rapid electrochemical detection. When DNA aptamers, previously selected for *B. cereus* spores, were immobilized on screen-printed gold electrodes, they exhibited higher binding capacity than individual aptamers, suggesting a synergistic effect. Additionally, the mixture of rhodamine-labelled aptamers enabled spatial fluorescent visualization of the *B. cereus* endospore structure, confirming the increased binding efficiency. The electrochemical aptasensor based on three aptamers exhibited a wide dynamic range (10^2–10^7 CFU/mL) and low limit of detection (~1 CFU/mL) using just 15 μL of sample. Validation in spiked salad, using direct spore sensing in rinse water and comparison with the culturing method, confirmed its sensitivity and specificity. These combined aptamer approaches, achieving rapid (15 min) and single-step detection may also be suitable for detecting other foodborne pathogens.

1. Introduction

The World Health Organization European Region estimates that more than 23 million people fall ill from eating contaminated food each year, resulting in 4654 deaths and over 400,000 disability-adjusted life years [1]. However, foodborne diseases are entirely preventable, and their burden can be reduced by strengthening prevention, surveillance and management of food safety risks. In addition to implementing strict hygiene regulations, developing innovative pathogen detection methods, that can be applied directly to food is critical to protect consumers and enhance global health security.

Among food contaminating agents, *Bacillus cereus,* a Gram-positive spore-forming bacteria, poses serious problems for both consumers and the food industry [2,3]. It is the primary microbe associated with baby food, the third most common agent responsible for collective foodborne outbreaks in Europe [4,5], and the third leading foodborne pathogen in China [6]. In the United States, 60,000 cases of foodborne diseases caused by *B. cereus* are reported annually [7]. *B. cereus,* also known as *Bacillus cereus sensus lato* (s.l.), can cause gastrointestinal diseases ranging from mild to severe, primarily through the production of enterotoxins and emetic toxins that cause diarrhea and emetic syndrome, respectively [4,8]. Moreover, *B. cereus* has been identified as the causing agent of systemic and localized infections, especially in high-risk populations, and in rare cases, of toxic shock syndrome affecting the central nervous system [5]. The most dangerous species of the *B. cereus* group is *Bacillus anthracis*, the etiologic agent of anthrax, which causes a highly lethal disease in both humans and animals [8].

B. cereus, is widely distributed in the environment and can contaminate any food primarily through soil and air [8]. In its natural biotopes, *B. cereus* is mainly present in the form of spores and biofilm [9]. Spores allow bacteria to persist for years or even decades under environmental stressors such as heat, dryness, UV radiation, and chemical disinfectants [9,10]. Spores are frequently detected in vegetation, waters, meat, eggs, milk, and processed food, where they can survive heat-treatments, such as pasteurization, which eliminate other microorganisms [11,12]. Then, when conditions are favorable, the spores of *B. cereus* germinate and outgrow, leading to deterioration of the organoleptic qualities of food or producing toxins that can enter the human or animal body via food.

Official techniques for diagnosing *B. cereus* are culture-based [3,13,14]. These techniques are often efficient but labor intensive and time

* Corresponding author.
E-mail address: jasmina.vidic@inrae.fr (J. Vidic).

https://doi.org/10.1016/j.talanta.2025.129147
Received 29 September 2025; Received in revised form 31 October 2025; Accepted 20 November 2025
Available online 24 November 2025

consuming. Initial results, obtained after 2–3 days, indicate the presence of presumptive *B. cereus* cells; however, confirmation of the specific strain involved may take more than one week [13]. Advanced techniques, such as PCR, mass spectrometry, microarray, and genomic sequencing are promising and relatively rapid but require purified genetic material, high technical skills, and expensive, intensive sample processing [13,15,16]. Moreover, these diagnostic protocols are not directly applicable to spores and require an additional step: induction of spore germination, followed by detection of the resulting vegetative cells [10]. Consequently, no culturing or molecular method is available for routine use to screen food for *B. cereus* spores. Nevertheless, various categories of advanced biosensors are currently under development [7,10,16–20]. Among these, aptamer-based sensing stands-out as one of the most promising strategies allowing efficient and specific targeting of whole bacterial spores. This is particularly promising because these biosensors are low-cost, easy-to-use and deployable throughout the food manufacturing chain.

Aptamers are short, single-stranded nucleic acid sequences capable of selective and specific binding to targets, generally due to their specific three-dimensional structure. They are generated *in vitro* through a process called SELEX (Systematic Evolution of Ligands by Exponential Enrichment) and represent a cheaper and reversible alternative to expensive immunoassays. Unlike antibodies, aptamers exhibit low immunogenicity, extended shelf-life, and are inexpensive and easy to produce [21,22]. However, despite their attractiveness as recognition elements, aptasensors are still in their early stages and require long-term investigation and optimization for real-life applications [23,24].

Aptamers selected against *B. cereus* spores can be integrated into diagnostic aptasensors that function without the need for spore germination or lysis. Several aptamers with high affinity and specificity for binding *B. cereus* spores have been selected using cell-SELEX and are available in the literature [7,17,25]. This ability to recognize binding sites on the surface of spores, rather than intracellular biomarkers, should significantly reduce analysis time, representing a major advantage for low-cost and rapid food diagnostics. Although the precise molecular targets of aptamers selected by cell-SELEX remain to be identified and validated, it is unlikely that they bind to the same target, given the organizational complexity of the endospore surface and the diversity of the 3D structures of published aptamers.

Therefore, we speculate, here, that using a combination of aptamers that recognize *B. cereus* spores will enable targeting of multiple epitopes at their surface, thereby providing enhanced diagnostic sensitivity. To test this, we evaluated three different aptamers that have been previously characterized for their binding to spores of various *B. cereus* strains, including *B. anthracis*, named BAS6 [20,25], Apt1 [17] and Apt2 [17]. We characterized their structural stability in solution, and demonstrated that they do not hybridize with each other. Binding assays were conducted to compare the signals generated by individual aptamers and aptamer mixtures upon binding to *B. cereus* spores. The mixtures or individual aptamers were then employed in an aptasensor for electrochemical detection of spores, and their sensitivity and limits of detection were compared. Finally, the applicability of the aptasensor incorporating the aptamer combination with the best analytical performance was demonstrated through the direct detection of spores in fresh salad samples, requiring minimal sample preparation and providing results within 15 min.

2. Materials and methods

2.1. Reagents and materials

All chemicals used in this work were of analytical grade. Potassium hexacyanoferrate (III) (ferricyanide), potassium hexacyanoferrate (II) trihydrate, absolute ethanol, sulfuric acid, 6-mercapto-1-hexanol (MCH), glutaraldehyde, potassium chloride (KCl), potassium phosphate (K_3PO_4) and Tris (2-carboxyethyl) phosphine hydrochloride (98 %, TCEP) were purchased from Sigma-Aldrich (France). 1,1,1,3,3,3-hexamethyldisilazane (HMDS ≥98 %) was purchased from Acros Organics (Geel, Belgium). Phosphate buffered saline (PBS), pH 7.4, was purchased from Lonza (Basel, Switzerland) and used as 1X. Three aptamer sequences were obtained from Eurofins Genomics SAS (Nantes, France). Table 1 summarizes the aptamer sequences used in this study. Their secondary structures were predicted using the mfold web server [26]. All aptamer sequences were purchased as unmodified oligomers, thiolated at the 5′end with a $HO(CH_2)_6SS(CH_2)_6(T)_5$ group, or modified with TexasRed at the 5′ end.

Upon arrival, the lyophilized pellet of modified aptamer was diluted to a 100 μM stock solution using Milli-Q water and stored at −20 °C until use. Screen Printed Gold Electrodes (GSPE), type BT220, were purchased from Metrohm-DropSens (France). Texas Red aptamer solutions were used at a final concentration of 500 nM.

2.2. Bacterial strains and growth conditions

The non-pathogenic *B. cereus* strain INRA-SV-S51 isolated from soil was used in this study. The *Bacillus subtilis* NDmed strain was used as a control. For routine growth, *B. cereus* was propagated in Luria-Bertani (LB) medium (1 % NaCl, 1 % tryptone, 0.5 % yeast extract) at 37 °C. For sporulation, bacterial cells were grown in sporulation medium HCT (0.7 % casein hydrolysate, 0.5 % tryptone, 0.68 % KH_2PO_4, 0.012 % $MgSO_4{\cdot}7H_2O$, 0.00022 % $MnSO_4{\cdot}4H_2O$, 0.0014 % $ZnSO_4{\cdot}7H_2O$, 0.008 % ferric ammonium citrate, 0.018 % $CaCl_2{\cdot}4H_2O$, 0.3 % glucose, pH 7.2) [27] at 30 °C, with rotary agitation set to 200 rpm.

2.3. UV melting experiments

Melting experiments were performed on a Jasco V-750ST UV–visible (UV–Vis) spectrophotometer. Samples of 1–2 μM DNA were prepared by dissolving the stock solution in a mixture of 70 mM potassium chloride and 20 mM potassium phosphate (pH 7.0). For each measurement, absorbance at 268 nm was recorded as a function of temperature (15–80 °C). The heating and cooling rate was 0.2 °C/min. The determined melting temperature (Tm) represents the average of the results obtained during the heating and cooling cycles.

2.4. Circular dichroism experiments

Each aptamer (0.5–1 μM) was dissolved in a mixture of 70 mM potassium chloride and 20 mM potassium phosphate (pH 7.0) and circular dichroism (CD) spectra were acquired at 20 °C using a Jasco J1500 spectropolarimeter. Spectra were recorded from 220 to 320 nm, at 200 nm/min. For each measurement, the average of 3 consecutive scans was taken, the buffer contribution was subtracted, and the data were zero-corrected at 320 nm.

2.5. Native gel electrophoresis

The DNA aptamer (1–2 μM) was dissolved in 70 mM potassium chloride-20 mM potassium phosphate (pH 7.0) mixture. Samples were loaded onto 20 % nondenaturing polyacrylamide gels that had been previously spiked with 50 % (v/v) glycerol. The gels were visualized by UV-shadowing.

2.6. Spectrophotometry

The binding of aptamers to spores of the *B. cereus* S51 strain was evaluated using a UV–Vis spectrophotometer Biochrom Libra S22 (Biochrom Ltd., Cambridge, UK). Spores (10^4 CFU/mL) were mixed with 5 μM aptamer in 10 mM Tris-HCl, pH 8 and incubated at 4 °C for 4 h with gentle shaking. The spores were then centrifuged at 3000 rpm for 5 min, washed three times and resuspended in 10 mM Tris-HCl, pH 8, for analysis. In control experiments, the aptamers were replaced with the

Table 1
Sequences of ssDNA used in this study.

Sequence (5' → 3')	Length	Calculated T_m(°C)	Experimental T_m(°C)	Reference
Apt1 CATCCGTCACACCTGCTCGGTGCAGACCCATAGGGGGGGCGTGCGGATGTGCGGAGTAGGGTGTTCGCTCCCGTATC	77mer	87.5 °C	50.7 ± 0.3	[17]
Apt2 CATCCGTCACACCTGCTCCCCAATGAAGCGAGATGGACGCCTAGCACCCCCCGCGTCCGGTGTTGGCTCCCGTATC	76mer	87.2 °C	41.9 ± 0.6	[17]
BAS6 ATCCGTCACACCTGCTCTGCACGGGCTCAGTTTGGCTTTGTATCCTAAGAGGATGGTGTTGGCTCCCGTAT	71mer	82.1 °C	31.8 ± 0.6	[25]

control oligomer sequence Campy (5′-GGGAGAGGCA-GATGGAATTGGTGGTGTAGGGGTAAAA TCCGTAGA-3′).

2.7. Construction of electrochemical aptasensor

The aptasensors were constructed using aptamer sequences modified at the 5′-end with Thiol-C_6-p$(T)_5$. The thiolated-aptamer working solution was prepared by mixing an aliquot of the 50 μM aptamer solution with an equal volume of 0.5 M TCEP, as described before [28–31]. The reaction was allowed to proceed for 1 h to ensure the complete reduction of disulphide bonds to thiol groups. The mixture was then passed through a Spin Desalting Column (7K MWCO, Thermo Scientific, France) and diluted to an aptamer concentration of 1 μM with PBS (pH 7.4) for use in the functionalization of the cleaned gold electrode surface. The SPGEs were functionalized with aptamers according to established procedures previously reported [32,33]. Prior to functionalization, the SPGE surface was cleaned electrochemically by performing cyclic voltammetry (CV) in 0.05 M H_2SO_4 in the potential range from 0 V to +1.1 V at the scan rate of 0.4 V/s (Fig. S1). A total of 50 repetitive scans was performed to ensure the cleanliness of the electrode surface, as demonstrated by the overlapping of consecutive cycles. Once the electrochemical cleaning was complete, the electrodes were thoroughly rinsed with Milli-Q water and dried. The electrodes were biofunctionalized immediately after the cleaning step by drop-casting 15 μL of the reduced 500 nM thiolated-aptamer solution. The electrodes were incubated for 1h at ambient temperature. The aptamer functionalized SPGEs were rinsed with PBS and incubated overnight at ambient temperature in 5 mM MCH solution prepared in PBS. Finally, the functionalized electrodes were copiously rinsed with Milli-Q water prior to electrochemical measurement. Different spore concentrations were incubated for 15 min prior to EIS measurement at room temperature. All electrode potentials are given versus the screen-printed quasi reference Ag/AgCl electrode.

2.8. Electrochemical measurements

All electrochemical measurements were performed using a portable PalmSens4 potentiostat/galvanostat/impedance analyzer (PalmSens BV, Netherlands), connected to a laptop equipped with PsTrace 5.11 software. Cyclic voltammetry (CV) measurements were conducted over a potential range from −0.4 to +0.5 V and at a scan rate of 100 mV/s, using PBS solution as a supporting electrolyte and 2.5 mmol/L of $[Fe(CN)_6]^{3-/4-}$ as the redox probe. Electrochemical impedance spectroscopy (EIS) measurements were recorded in the presence of 2.5 mmol/L $[Fe(CN)_6]^{3-/4-}$ as a redox probe in PBS. EIS was performed using the open circuit voltage (OCV) as the equilibrium potential by applying: 10 mV amplitude, number of frequencies: 71, maximum frequency: 10,000 Hz, minimum frequency: 1 Hz, min. sampling time: 0.5 s, max. equilibrium time: 5 s, OCP max. time was varying from 250 to 500 s for the different sensor layers, stability criterion: 0.001 mV/s. Subsequently, charge transfer resistance (R_{ct}) was determined by approximation based on calculating the diameter of the semi-circle of the real part of impedance [34]. The analytical plot was constructed using signal gain (R (%) = 100 × (R_{ct} sample− R_{ct} blank)/R_{ct} blank)) versus a logarithmic concentration range of *B. cereus* spores. The target detection limits (LoD) were calculated as three times the standard deviation of the blank divided with the slope of the obtained calibration curve, while limit of quantification (LoQ) was determined as a 3.3 time the LoD, according to the definition by the International Union of Pure and Applied Chemistry (IUPAC) [35].

2.9. Scanning electron microscopy

Functionalized SPGE carrying thiolated aptamers was incubated with 15 μL B. *cereus* spores water solution (10^4 CFU/mL) for 15 min at room temperature. Then, electrodes were washed with Milli-Q and mounted on aluminum stubs with carbon adhesive discs (Agar Scientific, Oxford Instruments SAS, Gomez-la-Ville, France). The surface was visualized by field emission gun scanning electron microscopy (SEM FEG) as secondary electron images (2 keV, spot size 30) under high-vacuum conditions with a Hitachi SU5000 instrument (Milexia, Saint-Aubin, France at facilities located on the MIMA2 platform, INRAE, Jouy-en-Josas, France).

Spores in solution were visualized using an Apreo 2C High-Resolution SEM (HRSEM; Thermo Fisher Scientific, Waltham, MA, USA). Samples were prepared following the previously described protocol [36]. Briefly, *B. cereus* and *B. subtilis* were suspended in PBS, centrifuged at 3000×*g* for 5 min and washed twice with PBS. Fixation was performed overnight at 4 °C using 2.5 % glutaraldehyde solution. Following fixation, the samples were centrifuged and the supernatants removed. The resulting bacterial pellets were deposited on sterile silicon wafers mounted on 32-mm aluminum stubs with carbon adhesive. Dehydration was achieved through a graded ethanol series (10 %–100 % in 10 % increments, 5 min per step). Subsequently, the samples were incubated for 5 min in a 1:1 ($_{v/v}$) mixture of ethanol and 50 % HMDS, followed by incubation in 100 % HMDS until complete evaporation. After air-drying, the samples were sputter-coated and imaged under HRSEM at an accelerating voltage of 2 keV and a probe current of 50 pA using an Everhart–Thornley detector (ETD).

2.10. Spores labelling using Texas Red-labelled aptamers

A volume of 99 μL of *B. cereus* spores (10^7 CFU/mL) was mixed with 1 μL of Texas Red-labelled aptamer sequences (100 μM) and incubated overnight at 4 °C under gentle shaking. After incubation, the samples were washed with PBS and precipitated by centrifugation five times at 3500 rpm for 3 min. The supernatant was removed by decantation, and the labelled spores were resuspended in PBS. A control sample containing *B. subtilis* spores at 10^7 CFU/mL was prepared using the same incubation method and washing steps.

2.11. Fluorescent microscopy

Images were acquired with an Axio-Observer Z1 inverted fluorescence microscope (Zeiss) equipped with an AxioCam 807mono digital camera (Zeiss) and fluorescence filters using a × 100 Apochromat objective (Zeiss). Stained spores were imaged using the 38 HE filter (excitation: BP 470/40, beam splitter: FT 495, emission: 525/50), and TexasRed was imaged using the 45 HE filter (excitation: BP 590/20, beam splitter: FT 605, emission: 620/14). Images were processed using

the ZEN software package (Zeiss) and ImageJ.

2.12. Spore contamination in ready-to-eat salad samples

A sample of the pre-washed salad (~50 g) was placed in a sterile Becher and inoculated with 1 mL of *B. cereus* spores water suspension (~10^3–10^5 CFU/mL). The salad was gently mixed and then flooded in 250 mL commercial mineral water for 15 min at 4 °C to simulate spore transfer. The transfer was performed at refrigerated temperature to mimic supermarket storage conditions and to prevent possible germination. Afterwards the salad was removed, and the spore containing water was collected and centrifuged. The pellet was resuspended in 1 mL fresh mineral water. The protocol aligns with established microbiological protocols for *B. cereus* food contamination modelling (Bacteriological Analytical Manual, BAM) [37]. Serial dilutions of the resulting spore-containing samples were analyzed using the aptasensors. In parallel, spore enumeration was performed by plate counting to evaluate biosensor performance. In control experiments, *B. cereus* spores were replaced with *B. subtilis* spores.

3. Results and discussion

3.1. Aptamer characterization

The originality of this work lies in the development of electrochemical aptasensors based on a mixture of aptamers targeting different epitopes on the surface of *B. cereus* spores in a non-competitive manner. The objective was to improve the electrochemical signal generated upon aptamer binding to captured spores by introducing multiple oligonucleotide sequences, compared to the traditional single-sequence approach. A gel migration assay showed that the Apt1, Apt2, and BAS6R aptamers (Table 1) do not bind to each other (Fig. 1a), thereby eliminating concerns about their spontaneous hybridization, which could compromise target recognition when these sequences are used in a mixture. In dilute solution (water solution containing 70 mM KCl), the CD spectra of the three aptamer sequences show a characteristic positive peak at 275 nm and a negative peak at 240 nm for folded DNA molecules (Fig. 1b). The folding was confirmed by 2D modelling of the three aptamers using the mfold software, which generated several possible structures for Apt1 and Apt2 and one for BAS6 (Fig. S1). The variability in conformations and loop sites of the three aptamers suggests that they may bind at different sites on the spore surface. However, the existence of multiple 2D structures for Apt1 and Apt2 can be a drawback for their applications, as only one conformation may possess the necessary recognition capability. In addition, UV melting experiments demonstrated that Apt1 and Apt2 were more stable than BAS6 which can be partially unfolded at the room temperature (Table 1). Considering that aptamer conformation is essential for target binding, the low thermal stability of BAS6 may compromise the accuracy and reproducibility of the sensors.

To confirm that the aptamers Apt1, Apt2, and BAS6 bind to spores of the *Bacillus cereus* strain, the spores were incubated with each aptamer and analyzed by UV–Vis spectroscopy. As nucleic acids, aptamers exhibit strong UV absorbance around 260 nm, whereas spores do not absorb significantly at this wavelength (Fig. 1c). However, when *B. cereus* spores were incubated with aptamers and thoroughly washed, a peak at 260 nm was observed, indicating aptamer binding (Fig. 1c). In contrast, no peak around 260 nm was detected when aptamers were incubated with unrelated spores of *B. subtilis*, suggesting no binding to the control and thus confirming the specificity of the interaction. The specificity was further confirmed by incubating *B. cereus* spores with the control oligonucleotide Campy, as no binding was observed in this case either (Fig. 1c). This set of experiments was performed in Tris buffer (pH 8), while Apt1 and Apt2 were selected in a sodium acetate buffer, pH 5 [17], and BAS6 in a Tris buffer containing NaCl and $MgCl_2$ salt, pH 7.5 [25]. It appears, therefore, that the functional structures of the aptamers remain active across a range of pH and salt concentrations.

3.2. Verification of aptamers' synergistic effect

To evaluate whether combining two or three aptamers yields a synergic effect and enhances affinity for *B. cereus* spore binding, aptamer molecules modified with the fluorescent reporter Texas Red were used for spore staining (Fig. 2a). After removal of unbound aptamers, the thoroughly washed spores were visualized by epifluorescence microscopy, and their staining intensity was analyzed using ImageJ. Ultrastructural visualization of *B. cereus* S51 spores revealed distinct morphological characteristics such as an ellipsoidal shape, typical length of 2–3 μm long, with a rugged coat and a prominent exosporium (Fig. 2b and S3). The obtained fluorescent imaging results suggest that the selected oligonucleotide sequences can bind both, the core and the exosporium of *B. cereus* spores (Fig. 2c and d). In particular, BAS6, alone or in a mixture, marked the exosporium, which is in line with our previous report on BAS6 interaction with *B. cytotoxicus* spores [19]. The binding of aptamers to the exosporium was confirmed by quantification through image analysis of the respective proportion of fluorescence in the stained spores (Fig. S4). The total molar concentration of each individual aptamer or their combinations (double or triple) was kept constant at 1 μM to allow comparison of fluorescence intensities. As shown in Fig. 2e, the lowest fluorescence was observed with Apt2, while other aptamers, alone or in mixtures, showed similar mean fluorescence intensity over the whole spore area. Accordingly, no synergistic effect, but rather a cumulative one, was observed when multiple aptamers bound to *B. cereus* spores. We next sought to verify whether aptamers can exhibit synergistic effects when immobilized on the electrode surface.

3.3. Fabrication and characterization of aptamer-modified electrodes

Fig. 3a illustrates the two-step fabrication process of the aptamer-modified SPGE and the spore capturing. First, the surface of the electrochemically cleaned SPGE was functionalized with the 5′-alkylthiolated-aptamer using the drop-casting method. This step enabled the formation of a self-assembled monolayer of aptamer molecules on the gold substrate. Previous studies have shown that long-chain alkylthiolates can be stably immobilized on the gold surface due to lateral van der Waals interactions between neighboring monolayer molecules [33,38]. In the second step, MCH was employed as a passivation molecule to block unoccupied areas of the gold surface following aptamer binding and to reduce nonspecific adsorption. In addition, MCH acted as a spacer between neighboring aptamer molecules to provide optimal aptamer-aptamer distance for sterically unimpeded binding events with the target spore [33]. The SPGE functionalization was characterized by CV using ferro/ferricyanide as the redox couple in PBS as the supporting electrolyte. Fig. S5 shows a gradual decrease in redox-peak current intensity and an increase in peak-to-peak separation following electrode incubation with aptamers and MCH. This indicates an increase in the charge transfer resistance of the ferro/ferricyanide species, due to the formation of the mixed monolayer. SEM visualization of the functionalized working electrode suggests the presence of an organic layer over the gold surface, with some defects due to the inherent roughness of the gold (Fig. 3b and Fig. S6). Indeed, the BSE mode for Z-contrast shows different signal intensities on the working electrode surface (Fig. S6), indicating the presence of organic matter which appears darker (low Z). Finally, to verify whether the attached aptamers retained their recognition capability, the functionalized electrode was incubated with *B. cereus* spores for 15 min, thoroughly washed, and then examined by SEM. Fig. 3c and Fig. S6 show that spores were indeed captured on the functionalized surface, indicating that the immobilized aptamer kept its functional conformation after immobilization.

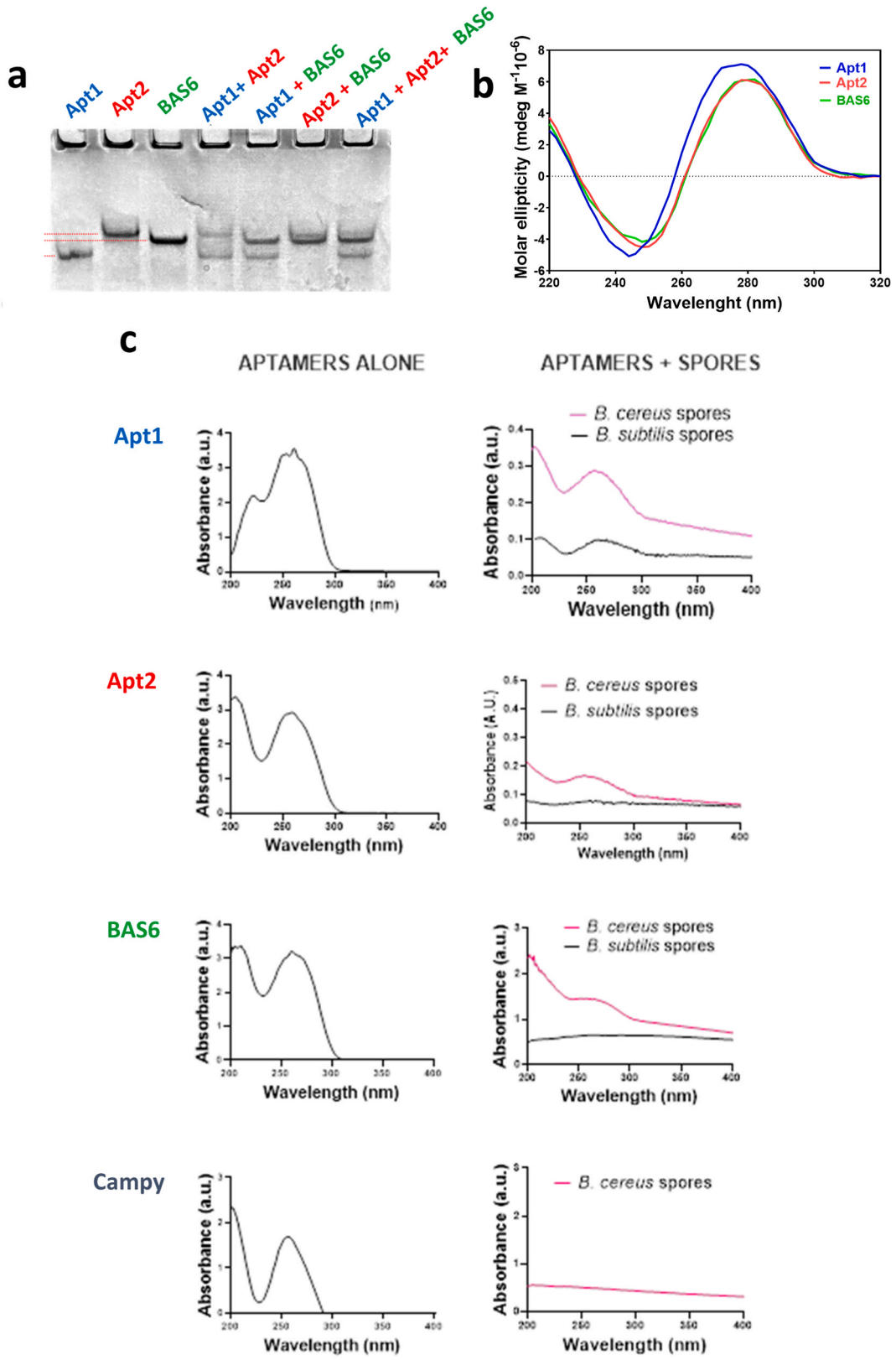

Fig. 1. (**a**) Native gel electrophoresis of different aptamer sequences and their mixtures. The names of the sequences loaded in the gels are listed above each well. (**b**) CD spectra of Apt1 (blue), Apt2 (red) and BAS6 (green). (**c**) Spectrophotometric detection of BAS6, Apt1 and Apt2 aptamer alone (left panel) and bound to spores of *B. cereus* or *B. subtilis* (right panel). Campy oligonucleotide was used as a negative control. Binding experiments were performed with 10^4 CFU/mL of spores and 10 μM aptamer.

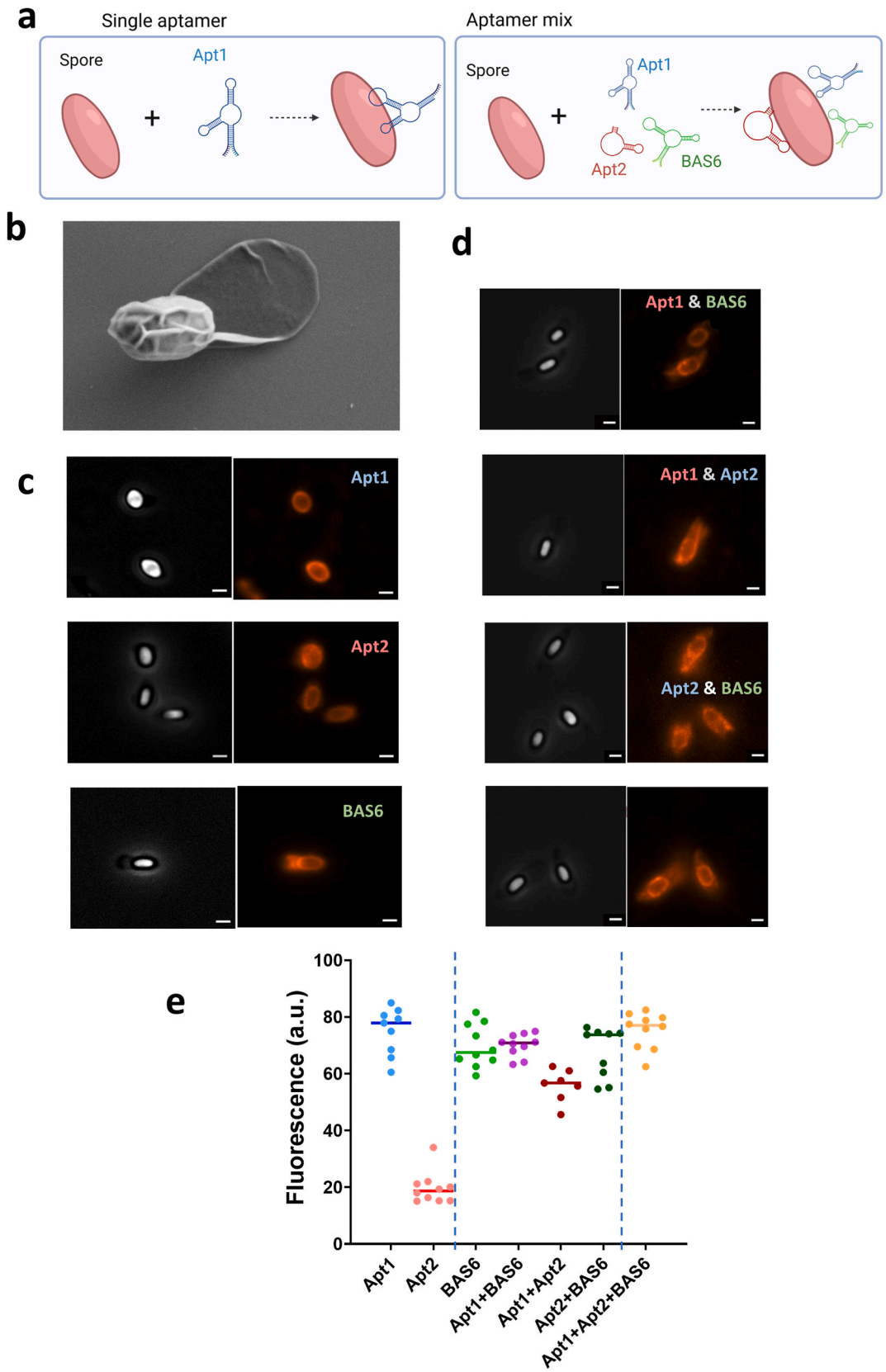

Fig. 2. (**a**) Schematic representation of the concept of signal enhancement by using aptamer mixtures for spore detection. (**b**) SEM visualization of B. cereus S51 spore. Scale bar, 1 μm. (**c**) Representative fluorescence images of *B. cereus* S51 spores stained with individual aptamers (1 μM) modified with Texas Red at 5'. Scale bar, 1 μm. Left panels show bright field images of spores. (**d**) Representative fluorescence images of *B. cereus* S51 spores stained with combinations (double or triple) of aptamers modified with Texas Red at the 5′ end. The total molar concentration of aptamers in mixtures was 1 μM. Left panels show bright field images of spores. Scale bar, 1 μm. (**e**) Scatter plot of fluorescence intensity per spore from at least 10 spores as in (**c, d**) determined by ImageJ software. The bar represents the median.

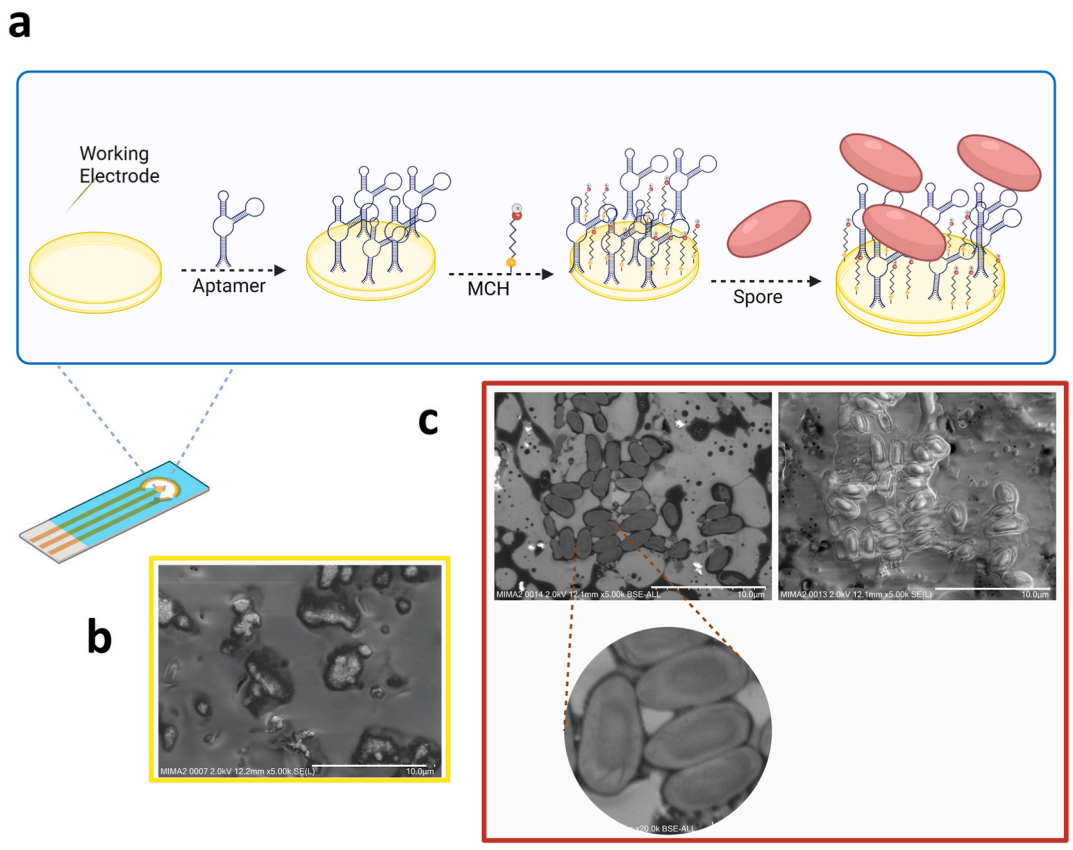

Fig. 3. (**a**) Schematic concept of SPGE functionalization by using aptamers and MCH, and subsequent spore sensing. (**b**) SEM image of the electrode functionalized with aptamer BAS6 and MCH. Scale bar, 10 μm. (**c**) SEM images of spores captured on the electrode surface functionalized with BAS6 aptamer and MCH. Scale bar, 10 μm.

3.4. Electrochemical detection of spores

The comparative detection test was performed with SPGEs functionalized with single or multiple aptamers (at constant total concentration of 1 μM) and exposed to 10^5 CFU/mL of *B. cereus* spores for 15 min. EIS was used to characterize spore binding in a solution of the 5 mM ferro/ferrycyanide in PBS. Fig. 4a shows the degree of signal gain for single, double, or triple aptamers, calculated for charge transfer resistance R_{ct}. R_{ct} reflects modification of the electrode surface due to target capture by the aptamer molecules on the electrode surface, as it depends on the dielectric and insulating properties at the electrode/electrolyte interface. A clear synergistic effect was observed with electrodes carrying double Apt1+BAS6 and triple Apt1+BAS6+Apt2 aptamers, which provided a significant enhancement of signal gain compared to single aptamers or doubles involving Apt2.

Fig. 4b shows a series of Nyquist plots recorded in a solution containing increasing concentrations of *B. cereus* spores. The obtained data were fitted using an equivalent circuit shown in the inset of Fig. 4b and the corresponding R_{ct} values were calculated. A linear increase in R_{ct} value was observed with increasing the spore concentration from 10^2 to 10^7 CFU/mL. As expected, the best analytical properties were obtained with SPGE functionalized with the triple aptamers, which exhibited increased signal gain across all individual aptamers. The total molar concentration of each individual aptamer or their combinations (double or triple) was kept constant at 1 μM to allow comparison of signal gains. The triple-aptamer biosensor showed an (R^2) of 98.5 % and the regression equation $y = 4.075\,x + 2.24$, where x is log (spore concentration in CFU/mL), y is signal gain, % (Fig. 4c). The calculated limit of detection (LoD) was 1.26 CFU/mL while the limit of quantification (LoQ) was 4.16 CFU/mL when detection was performed with three-aptamer electrodes. LoD and LoQ values for other sensors are presented in Fig. 4d. For comparison, a previously reported impedimetric biosensor employing BAS6R as a sensing element showed a much shorter linear range between 10^4 CFU/mL–5×10^6 CFU/mL and a detection limit of more than 1000 CFU/mL [20]. The improved analytical performance of the aptasensor based on three aptamers compared to corresponding individual aptasensors confirms our hypothesis that Apt1, Apt2 and BAS aptamers target distinct, non-overlapping epitopes on the spore surface. The triple-aptamer used in the electrochemical aptasensor, which exhibited the highest efficiency and was further employed for spore detection in a food sample.

3.5. Detection of B. cereus spores in ready-to-eat salad samples

To ensure the analytical reliability of the triple-aptamer electrochemical aptasensor, its performance was validated through a study using spiked green salad. To mimic a real-world contamination scenario, ready-to-eat salad samples were inoculated with known concentrations of *B. cereus* spores (10^1 CFU/mL - 10^7 CFU/mL), soaked in commercial mineral water to simulate the washing step, and the resulting effluent wash-water was analyzed by the triple-aptamer aptasensor (Fig. 5a and Fig. S7). Maeasurements were performed in a solution of the ferro/ferrycyanide redox couple that has been prepared in mineral water. The corresponding Nyquist plots of the impedance spectra are shown in Fig. 5b. Controls performed with *B. subtilis* spores showed significantly smaller variations in Nyquist plots (Fig. 5c). The fitting of the spectra was as satisfactory as that reported in Fig. 4b for PBS as a supporting electrolyte. Fig. 5d shows the calibration curve obtained from quantification of the signal gain for *B. cereus* spores for each spore concentration. The obtained R_{ct} values present the average of three independent sensors with the relative standard deviation of ca. 4 %. Signal gains plotted against the logarithm of target spore concentrations

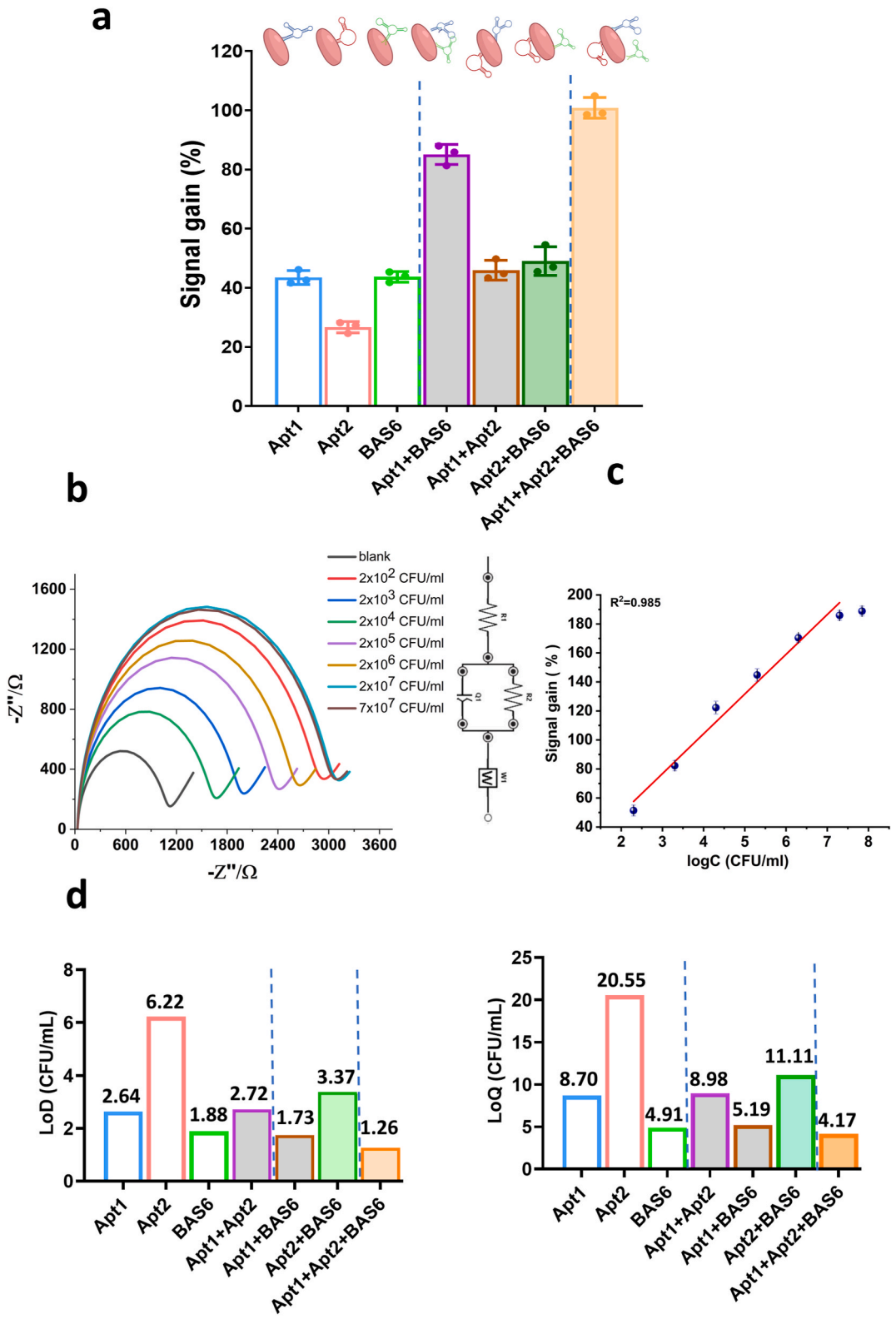

Fig. 4. (**a**) Signal gain calculated as 100 × ((R_{ct} sample− R_{ct} blank)/R_{ct} blank) of *B. cereus* spores obtained by the electrochemical biosensor based on single, double or triple aptamers for the same concentration of the 10^5 CFU/mL. The total aptamer concentration (single, double, or triple) was maintained at 1 μM. In all cases, the spores were incubated with the modified electrodes for 15 min. (**b**) Nyquist plots of impedance spectra taken in PBS with ferro/ferri cyanide redox couple in PBS with various concentrations of *B. cereus* spores using the triple-aptamer aptasensor. Inset: the equivalent circuit used for fitting impedance spectra. (**c**) Corresponding calibration curves obtained by plotting the signal gain as a function of *B. cereus* spore concentrations. Data points are mean values obtained in 3 independent experiments ± SD. (**d**) LoD and LoQ of *B. cereus* spore detection by single or multiple aptamers immobilized on an SPGE.

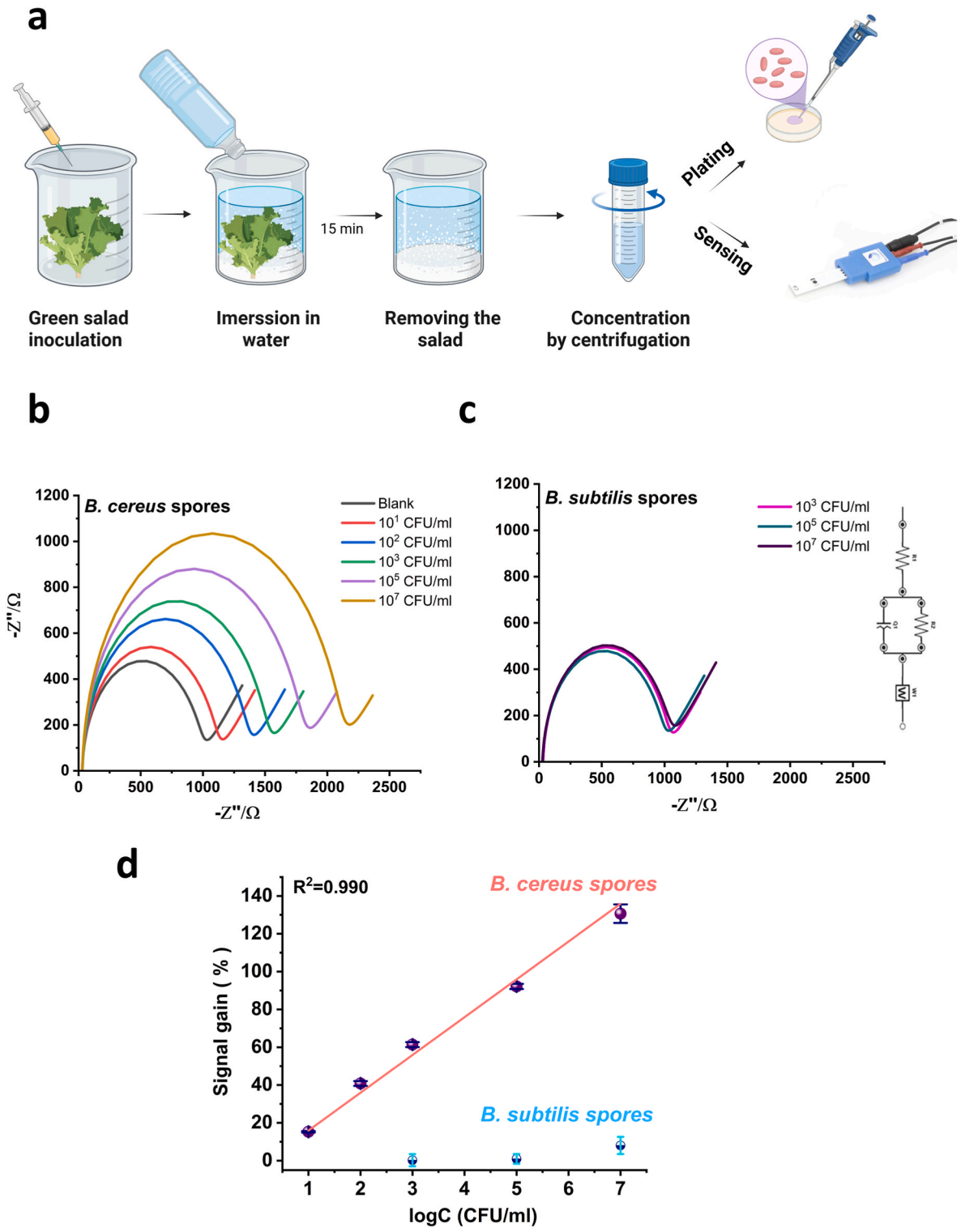

Fig. 5. (**a**) Schematic representation of the triple-aptamer based assay building protocol applied to detect *B. cereus* spore in contaminated ready-to-eat salad samples. To mimic a real-world contamination scenario, ready-to-eat salad samples were inoculated with known concentrations of *B. cereus* spores, soaked in commercial mineral water to enable transfer and tested by the aptasensor. Results were verified with plating experiments. Nyquist plots of impedance spectra recorded with ferro/ferri cyanide redox couple in mineral water with various concentrations of *B. cereus* spores (**b**) or *B. subtilis* spores (**c**) using the triple-aptamer aptasensor. Insert, the equivalent circuit used for fitting impedance spectra. (**d**) Calibration curves were obtained by plotting the signal gain in a function of *B. cereus* and *B. subtilis* spore concentrations. Data points are the mean values obtained in 3 independent experiments ± SD.

were linear with a correlation coefficient (R^2) of 99 % and the following regression equation: $y = 5.46\ x + 1.70$. For comparison, an insignificant variation in signal gain was observed when the triple-aptamer aptasensor was tested with the same range of concentrations of *B. subtilis* spores used as a negative control (Fig. 5d), confirming the sensor high selectivity towards *B. cereus* spores. Interestingly, due to the better conductivity of mineral water compared to PBS, the sensitivity of detection in rinse water was exceptional with LoD of 0.9373 CFU/mL

and LoQ of 3.0933 CFU/mL. Together, the specificity and selectivity of *B. cereus* spore detection from inoculated salads strongly suggest the reliability of the triple-aptamer aptasensor for food safety screening.

4. Conclusion

The combination of three aptamers and an impedance-based detection strategy was presented in this study as a novel approach for the diagnosis of *B. cereus* spores directly from food samples, without the need for bacterial enrichment, culturing, or biomarker purification. The use of an aptamer mixture effectively increased the sensitivity of electrochemical spore detection compared to single aptamer. This finding suggests that lateral interactions between aptamers within the monolayer formed on the gold electrode surface may play an important role in aptasensor stability and efficiency. The method enabled rapid and ultrasensitive detection of *B. cereus* spores at concentrations as low as 1–2 CFU/mL within 15 min. This triple-aptamer aptasensor has the potential to be used by the food industry and regulatory agencies to monitor food quality, especially considering that different *B. cereus* strains can cause food spoilage, gastrointestinal diseases, and infections. The results support the use of aptamer mixtures for the detection of targets exposing multiple epitopes, such as bacteria or eukaryotic cells.

CRediT authorship contribution statement

Milica Sentic: Writing – review & editing, Visualization, Investigation, Formal analysis. **Francesco Rizzotto:** Writing – review & editing, Investigation, Formal analysis. **Zorica Novakovic:** Writing – review & editing, Formal analysis. **Aleksandar Karajic:** Writing – review & editing. **Brahim Heddi:** Writing – review & editing, Resources, Investigation. **Jasmina Vidic:** Writing – review & editing, Writing – original draft, Funding acquisition, Conceptualization.

Declaration of competing interest

The authors declare that they have no known competing financial interests or personal relationships that could have appeared to influence the work reported in this paper.

Acknowledgments

This work was supported in part by the French National Agency for Research (ANR-21-CE21-0009 Siena) and the European Union (grant agreement no. 101135402, Mobiles project and grant agreement no. 872662, IPANEMA project). M.S. acknowledges the support of the Ministry of Science, Technological Development and Innovation of the Republic of Serbia, Contract No: 451-03- 136/2025-03/200026. We thank Thierry Meylheuc for its expertise and the MIMA2 platform for access to electron microscopy equipment (MIMA2, INRAE, 2018. Microscopy and Imaging Facility for Microbes, Animals and Foods, https://doi.org/10.15454/1.5572348210007727E12).

Appendix A. Supplementary data

Supplementary data to this article can be found online at https://doi.org/10.1016/j.talanta.2025.129147.

Data availability

Data will be made available on request.

References

[1] WHO. http://www.euro.who.int, 2025.
[2] E.F.S. Authority, The European Union one health 2018 zoonoses report, EFSA J. 17 (12) (2019) e05926.
[3] J. Jovanovic, et al., Bacillus cereus food intoxication and toxicoinfection, Compr. Rev. Food Sci. Food Saf. 20 (4) (2021) 3719–3761.
[4] N. Ramarao, et al., Advanced methods for detection of Bacillus cereus and its pathogenic factors, Sensors 20 (9) (2020) 2667.
[5] D. Cormontagne, et al., Bacillus cereus induces severe infections in preterm neonates: implication at the hospital and human milk bank level, Toxins 13 (2) (2021) 123.
[6] N. Paudyal, et al., A meta-analysis of major foodborne pathogens in Chinese food commodities between 2006 and 2016, Foodborne Pathogene Dis. 15 (4) (2018) 187–197.
[7] Z. Zhou, et al., Portable dual-aptamer microfluidic chip biosensor for Bacillus cereus based on aptamer tailoring and dumbbell-shaped probes, J. Hazard Mater. 445 (2023) 130545.
[8] M. Ehling-Schulz, D. Lereclus, T.M. Koehler, The Bacillus cereus group: bacillus species with pathogenic potential, Microbiol. Spectr. 7 (3) (2019), https://doi.org/10.1128/microbiolspec.gpp3-0032-2018.
[9] Y. Huang, S.H. Flint, J.S. Palmer, Bacillus cereus spores and toxins–the potential role of biofilms, Food Microbiol. 90 (2020) 103493.
[10] J. Vidic, et al., Food sensing: detection of Bacillus cereus spores in dairy products, Biosensors 10 (3) (2020) 15.
[11] A. Soni, et al., Bacillus spores in the food industry: a review on resistance and response to novel inactivation technologies, Compr. Rev. Food Sci. Food Saf. 15 (6) (2016) 1139–1148.
[12] P. Setlow, Spores of bacillus subtilis: their resistance to and killing by radiation, heat and chemicals, J. Appl. Microbiol. 101 (3) (2006) 514–525.
[13] J. Vidic, et al., Point-of-need DNA testing for detection of foodborne pathogenic bacteria, Sensors 19 (5) (2019) 1100.
[14] F. Rizzotto, et al., Recent advances in electrochemical biosensors for food control, Micromachines 14 (7) (2023) 1412.
[15] E. Gerace, et al., Recent advances in the use of molecular methods for the diagnosis of bacterial infections, Pathogens 11 (6) (2022) 663.
[16] A. Ait Lahcen, et al., Label-free electrochemical sensor based on spore-imprinted polymer for Bacillus cereus spore detection, Sensor. Actuator. B Chem. 276 (2018) 114–120.
[17] C. Fischer, et al., Food sensing: aptamer-based trapping of Bacillus cereus spores with specific detection via real time PCR in milk, J. Agric. Food Chem. 63 (36) (2015) 8050–8057.
[18] C. Park, et al., Detection of Bacillus cereus using bioluminescence assay with cell wall-binding domain conjugated magnetic nanoparticles, BioChip J. 12 (2018) 287–293.
[19] F. Rizzotto, et al., Colorimetric aptasensor for detection of Bacillus cytotoxicus spores in milk and ready-to-use food, Heliyon 9 (7) (2023) e17562.
[20] V. Mazzaracchio, et al., A label-free impedimetric aptasensor for the detection of Bacillus anthracis spore simulant, Biosens. Bioelectron. 126 (2019) 640–646.
[21] V. Léguillier, B. Heddi, J. Vidic, Recent advances in aptamer-based biosensors for bacterial detection, Biosensors 14 (5) (2024) 210.
[22] M. Manceau, et al., Investigation of the affinity of aptamers for bacteria by Surface plasmon resonance imaging using nanosomes, ACS Appl. Mater. Interfaces 16 (23) (2024) 29645–29656.
[23] A. Brown, et al., Development of better aptamers: structured library approaches, selection methods, and chemical modifications, Angew. Chem. Int. Ed. 63 (16) (2024) e202318665.
[24] J. Nourry, et al., Study of interactions between aptamers/antibodies and bacteria, in: International Oligonucleotides and Peptides Conference, 2024.
[25] J.G. Bruno, M.P. Carrillo, Development of aptamer beacons for rapid presumptive detection of bacillus spores, J. Fluoresc. 22 (2012) 915–924.
[26] M. Zuker, Mfold web server for nucleic acid folding and hybridization prediction, Nucleic Acids Res. 31 (13) (2003) 3406–3415.
[27] M.-M. Lecadet, M.-O. Blondel, J. Ribier, Generalized transduction in Bacillus thuringiensis var. berliner 1715 using bacteriophage CP-54Ber, Microbiology 121 (1) (1980) 203–212.
[28] R.M. Bakestani, et al., Carboxylate-terminated electrode surfaces improve the performance of electrochemical aptamer-based sensors, ACS Appl. Mater. Interfaces 17 (5) (2025) 8706–8714.
[29] M. Friedel, et al., Continuous molecular monitoring of human dermal interstitial fluid with microneedle-enabled electrochemical aptamer sensors, Lab Chip 23 (14) (2023) 3289–3299.
[30] A.M. Downs, et al., Subsecond-resolved molecular measurements using electrochemical phase interrogation of aptamer-based sensors, Anal. Chem. 92 (20) (2020) 14063–14068.
[31] V. Clark, et al., Extending the operational lifespan of nucleic acid-based electrochemical sensors via protection against hydrogen peroxide and oligonucleotide displacement, ACS Sens 10 (2025) 4945–4953.
[32] Y. Xiao, R.Y. Lai, K.W. Plaxco, Preparation of electrode-immobilized, redox-modified oligonucleotides for electrochemical DNA and aptamer-based sensing, Nat. Protoc. 2 (11) (2007) 2875–2880.
[33] Z. Watkins, et al., Week-long operation of electrochemical aptamer sensors: new insights into self-assembled monolayer degradation mechanisms and solutions for stability in serum at body temperature, ACS Sens. 8 (3) (2023) 1119–1131.
[34] E.P. Randviir, C.E. Banks, A review of electrochemical impedance spectroscopy for bioanalytical sensors, Anal. Methods 14 (45) (2022) 4602–4624.
[35] G.L. Long, J.D. Winefordner, Limit of detection. A closer look at the IUPAC definition, Anal. Chem. 55 (7) (1983) 712A–724A.

[36] E.N. Grafskaia, et al., Non-toxic antimicrobial peptide Hm-AMP2 from leech metagenome proteins identified by the gradient-boosting approach, Mater. Des. 224 (2022) 111364.

[37] S.M. Tallent, et al., BAM Chapter 14: Bacillus Cereus, Bacteriological analytical manual, 1998.

[38] C.D. Bain, et al., Formation of monolayer films by the spontaneous assembly of organic thiols from solution onto gold, J. Am. Chem. Soc. 111 (1) (1989) 321–335.